Nonmonotonic incommensurability effects in lamellar-in-lamellar self-assembled multiblock copolymers

Kriksin, Yury A.; Erukhimovich, Igor Ya.; Smirnova, Yuliya G.; Khalatur, Pavel G.; ten Brinke, Gerrit

Published in:
Journal of Chemical Physics

DOI:
10.1063/1.3138903

Publication date:
2009

Nonmonotonic incommensurability effects in lamellar-in-lamellar self-assembled multiblock copolymers

Yury A. Kriksin,[1] Igor Ya. Erukhimovich,[2,a)] Yuliya G. Smirnova,[3] Pavel G. Khalatur,[2] and Gerrit ten Brinke[3]
[1]*Institute for Mathematical Modeling, RAS, Moscow 125047, Russia*
[2]*Institute of Organoelement Compounds, RAS, Moscow 119991, Russia*
[3]*Laboratory of Polymer Chemistry, Zernike Institute for Advanced Materials, University of Groningen, Nijenborgh 4, 9747 AG Groningen, The Netherlands*

(Received 17 December 2008; accepted 17 April 2009; published online 26 May 2009)

Using the self-consistent-field theory numerical procedure we find that the period D of the lamellar-in-lamellar morphology formed in symmetric multiblock copolymer melts $A_{mN/2}(B_{N/2}A_{N/2})_nB_{mN/2}$ at intermediate segregations changes nonmonotonically with an increase in the relative tail length m. Therewith D reveals, as a function of the Flory χ-parameter, a drastic change in the vicinity of the internal structure formation, which can be both a drop and a rise, depending on the value of m. It is argued that the unusual behavior found is a particular case of a rather general effect of the incommensurability between the two length scales that characterize the system under consideration. © *2009 American Institute of Physics*. [DOI: 10.1063/1.3138903]

I. INTRODUCTION

The effects of incommensurability are observed when a system, which in bulk would self-assemble in a crystal lattice of a period L, is ordering in a confined volume whose characteristic size D is not divisible by L. In particular, the period and morphology of the microdomains formed in block copolymers confined between plane hard walls or within cylindrical pores are clearly shown to differ from those in the bulk (see reviews[1–3] and references therein for the latest theoretical activity in the field; see also Refs. 4–6 and references therein).

The purpose of our paper is to present a new peculiar incommensurability effect in multiblock copolymer melts of two-length-scale architecture, which are capable of forming morphologies characterized by two scales [typically the morphologies are so-called lamellar-in-lamellar (LL) ones].

The LL morphologies were first observed experimentally in self-assembled comb-shaped supramolecules obtained by hydrogen bonding of pentadecyl phenol (PDP) short chain molecules to the poly(4-vinyl pyridine) block of a diblock copolymer of poly(4-vinyl pyridine) and polystyrene (PS-*b*-P4VP) (Refs. 7–12; see also Refs. 13–20). Typically, first the PS blocks microphase separate from P4VP(PDP) forming a lamellar morphology; on further cooling another comparatively short-length-scale lamellar structure is formed in the P4VP(PDP) domains due to microphase separation between the pentadecyl tails and the rest of the P4VP(PDP) hydrogen-bonded complex. In these systems the short-length-scale lamellar structure is oriented perpendicular (or perhaps with some tilting) to the large-length-scale structure. This short-length-scale structure is formed below approximately 67 °C inside the pre-existing large-length-scale structure, and although there is interplay between the two length scales, the large length scale is not affected much.

Inspired by the experimental observations on various PS-*b*-P4VP(PDP) systems, theoretical efforts were started to address self-assembly in two-length-scale block copolymer systems.[21–29] We found that the linear multiblock copolymers with two end blocks, which are relatively long compared to the repeating diblocks forming the middle multiblock, also exhibit two-length-scale self-assembly even if only two chemically different monomers are involved. Concrete multiblock copolymer systems that have been studied theoretically in some detail are of the form A-b-$(B$-b-$A)_n$-b-B, A-b-$(B$-b-$A)_n$-b-B-b-A, and C-b-$(A$-b-$B)_n$-b-A-b-C. The first two examples involve only two chemically different monomers, whereas the last one involves three different monomers. Experimentally representatives of these classes of multiblock copolymers have been studied by Matsushita and co-workers.[13–16] During recent years our theoretical efforts concerned in particular the LL structure of these systems in the strong segregation regime where both the long and short blocks are completely segregated. Obviously, in this case two types of domains are formed: (i) the thick domains filled basically by the long tails and (ii) the thin domains filled exclusively by the short blocks. In this respect the binary and ternary systems are essentially different as illustrated below by comparing the situation with a minimal number of internal layers with that with a maximal number of internal layers. Indeed, starting from a minimal number of internal layers in the ternary system, further stretching of the chains will result in the increase in the number of internal layers from three up to a maximum of $2n+1$. Therewith, the volume of the short-length-scale domains does not change during this stretching. The situation for the binary system A-b-$(B$-b-$A)_n$-b-B-b-A is very different; complete stretching will lead from a minimum of one internal layer to a maximum of $2n+1$ ones and an accompanied doubling of the

a)Electronic mail: ierukhs@polly.phys.msu.ru.

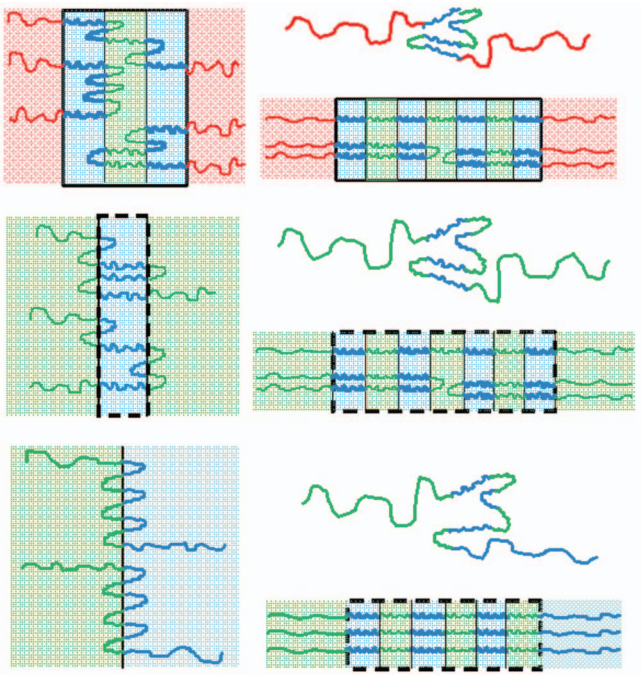

FIG. 1. (Color) Schematic illustration of the minimal and maximal numbers of internal layers for different multiblock copolymer systems. Top: C-b-$(B$-b-$A)_n$-b-B-b-C; middle: A-b-$(B$-b-$A)_n$-b-B-b-A; and bottom: A-b-$(B$-b-$A)_n$-b-B.

volume of the short-length-scale domains. An even more extreme situation is encountered for the system A-b-$(B$-b-$A)_n$-b-B. Here the minimal number of thin layers is simply zero, whereas on complete stretching $2n$ internal layers are formed. These differences are illustrated in Fig. 1.

The difference in behavior between the ternary and the binary systems is due to the fact that in the latter case, short A-(B-)blocks of the middle multiblock may be partly present in the thick A-(B-)layers as well. This has a strong influence on the equilibrium number of internal layers formed.[27–29] An increase in the number of internal layers for A-b-$(B$-b-$A)_n$-b-B or A-b-$(B$-b-$A)_n$-b-B-b-A generally leads to an increase in the amount of A/B interface, whereas for the ternary C-b-$(A$-b-$B)_n$-b-A-b-C systems this is not the case. Minimization of the interfacial area is an important driving force for block copolymer self-assembly, and, indeed, we recently observed that in the strong segregation limit an *increase* in the A/B incompatibility for LL self-assembled A-b-$(B$-b-$A)_n$-b-B-b-A multiblock copolymers results in a *reduction* in the number of internal layers.[28] An important element in the analysis turned out to be the (unfavorable) free energy contribution associated with the bimodal brushlike character of the "thick" end-block layers, which essentially consist of a mixture of "long" end-block tails and "short" chemically identical loops.[28]

The discussion above refers to the strong segregation situation where the LL structure is already present. At smaller A/B incompatibilities in A-b-$(B$-b-$A)_n$-b-B multiblock copolymer melts, we first have microphase separation between the end blocks only, whereas the middle multiblock is equally present in both layers. Increasing the incompatibility (lowering the temperature or increasing the lengths of the

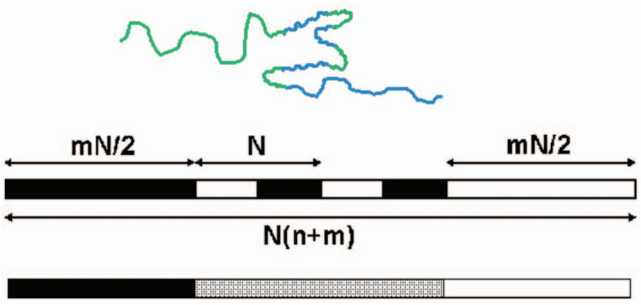

FIG. 2. (Color) Top: cartoon of $A_{mN/2}(B_{N/2}A_{N/2})_nB_{mN/2}$ multiblock copolymer; middle: parameter definition; and bottom: middle multiblock acts as a gray C-block characterized by an average incompatibility with respect to both the "white" end block and the "black" end block.

symmetric diblocks forming the middle multiblock) results in the additional formation of the internal layers. The interplay between the periodicity scales arising at the first stage (weak segregation) and the second one (intermediate segregation) is expected to cause new incommensurability effects. Indeed, such an effect was found by Nap *et al.*,[26] who studied the LL morphology at intermediate segregation in the melt of $A_{20}(BA)_{10}$ macromolecules consisting of a succession of ten symmetric diblock copolymer fragments A_dB_d (d is the degree of polymerization of one block) and a long tail A_{20d} via the self-consistent-field theory (SCFT) as developed by Matsen and co-workers.[30,31] It was shown that for increasing value of the χ parameter, the equilibrium composition profiles in such a melt become double periodic, thus indicating the forming of the LL morphology in qualitative accordance with the experimental findings by Matsushita *et al.*[13,14] Moreover, Nap *et al.*[26] found that unlike the situation for conventional diblock copolymer melts, the large period L characterizing the LL structure is not a monotonically increasing function of the incompatibility parameter χ.

It is this effect that we address in the present paper in more detail. We will show that around the temperature of the formation of the short-length-scale layers inside the existing lamellar morphology, the overall periodicity may suddenly increase or decrease up to 20% depending on the length of the end blocks. The case is that incommensurability of the two length scales involved forces the system to select between two options upon formation of the internal layers: either (i) the number of internal layers is too small and a *collapse* of the overall periodicity occurs, or (ii) the number of internal layers is too large and the system exhibits a sudden *swelling*. Of course, the system will select one of these two possibilities based on the lowest free energy.

II. MODEL AND METHOD

In this paper we study systematically the formation of the LL morphology in one specific class of systems with a two-length-scale architecture denoted as $A_{mN/2}(B_{N/2}A_{N/2})_nB_{mN/2}$ and shown in Fig. 2. These linear chains consist of two long A and B end blocks connected by a sequence of n repeating symmetric diblocks $B_{N/2}A_{N/2}$, where N, nN, $mN/2$, and $N_{tot}=(m+n)N$ are the degrees of polymerization of the elementary diblock, the middle multiblock part, the tails and the whole chain, respectively.

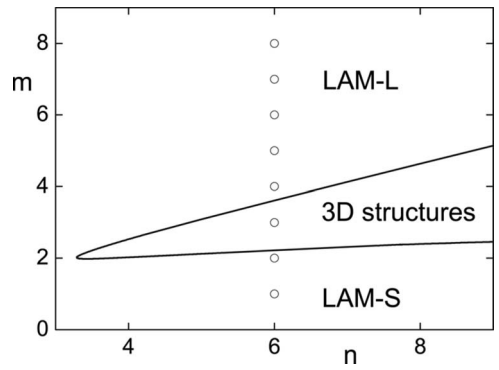

FIG. 3. The phase diagram of the multiblock copolymer melt under consideration. The solid line is calculated within the WST approach and delineates the regions of stability of the lamellar and different cubic morphologies (Ref. 24). The open circles correspond to the values of the structural parameters (n,m) for which the SCFT calculations are carried out. Letters L and S label the regions corresponding to the lamellar structures with large and small length scales, respectively.

Due to the very symmetry of the chosen class of AB copolymer melts, ordering (microphase separation) for this class is shown[23–25] at the mean-field level of the weak segregation theory (WST) to occur as a second order phase transition, i.e., continuously with decrease in temperature, which is similar to that in symmetric diblock copolymer melts.[32] The peculiar feature for the two-length-scale architecture block copolymer melts is that near the order-disorder transition (ODT) point, the period D of the lamellar structure formed depends strongly on the value of the ratio $\beta=m/n$, which characterizes the relative total length of the end blocks (tails) as compared to that of the middle multiblock part. The quantitative distinction between the different situations was given within the WST via analyzing the behavior of the structure factor and so-called fourth vertex.[24] The result is presented in Fig. 3, where some tiny regions, in which two-periodic noncubic morphologies are stable,[33] are disregarded.

If β is small enough (this region is labeled in Fig. 3 as LAM-S), then the lamellar period D is close to the that formed by the middle polyblock part $(B_{N/2}A_{N/2})_n$ only, i.e., $D\sim R_G^{\mathrm{di}}$, where $R_G^{\mathrm{di}}=a\sqrt{N/6}$ is the radius of gyration of one repeating diblock. On the other hand, if β is large enough (this region is labeled in Fig. 3 as LAM-L), then $D\sim R_G^{\mathrm{tot}}$, where $R_G^{\mathrm{tot}}=a\sqrt{N_{\mathrm{tot}}/6}$ is the radius of gyration of the whole chain. For intermediate values of β, the WST predicts[23–25] ordering into certain cubic phases rather than the lamellar one.

In the region LAM-L the system under consideration first (near the ODT) segregates on a large scale, in which case the middle AB (black-white) multiblock part behaves as a sort of "gray" block characterized by an average value of the solubility parameter. Accordingly, the phase behavior of such two-scale AB multiblock copolymers close to their critical point[23–25] resembles that of the ABC triblock copolymers,[34,35] whereas further increase in the χ-parameter characterizing the incompatibility of the A and B blocks is expected to result in additional short range segregation between the A and B blocks forming the middle gray part.

In this paper we focus on LL ordering at lower temperatures in the region LAM-L, for which purpose we apply the SCFT technique as described in detail in Refs. 26, 30, 31, 36, and 37. It is worth reminding now the basics of the SCFT procedure.

The free energy of the incompressible melt of flexible AB copolymers is

$$\mathcal{F}(\{\psi_A\},\{\psi_B\})/T=\int d^3\mathbf{r}[-f_A\psi_A(\mathbf{r})-(1-f_A)\psi_B(\mathbf{r}) + (\psi_A(\mathbf{r})-\Psi_B(\mathbf{r}))^2/(4\chi\mathcal{N})] - V\ln Q(\{\psi_A\},\{\psi_B\}). \quad (1)$$

Here V is the system volume; f_A is the average volume fraction of type A blocks $(f_A+f_B=1)$; $\psi_i(\mathbf{r})$ is the external field acting on the monomer of the ith type located at the point $\mathbf{r}$, the temperature T is measured in the energetic units, in which the Boltzmann constant $k_B=1$, and the single-chain partition function Q reads

$$Q(\{\psi_A,\psi_B\})=V^{-1}\int d^3\mathbf{r}q(\mathbf{r},1;\{\psi_A,\psi_B\}). \quad (2)$$

The end-to-end distribution function $q(\mathbf{r},s)\equiv q(\mathbf{r},s;\{\psi_A,\psi_B\})$ (non-normalized statistical weight) is defined by the modified diffusion equation

$$\partial q(\mathbf{r},s)/\partial s=R_G^2\nabla^2 q(\mathbf{r},s)-\psi(\mathbf{r},s)q(\mathbf{r},s), \quad (3)$$

with the initial condition $q(\mathbf{r},0)=1$ and

$$\psi(\mathbf{r},s)=\sigma_A(s)\psi_A(\mathbf{r})+\sigma_B(s)\psi_B(\mathbf{r}). \quad (4)$$

Here $\sigma_i(s)=1$ if the chain contour position s is occupied by the segment of the type i and $\sigma_i(s)=0$ otherwise.

The desired free energy is the saddle point value of the functional $\mathcal{F}[\psi_A,\psi_B]$ to be obtained via minimization of the latter with respect to the exchange potential

$$\psi_-(\mathbf{r})=\tfrac{1}{2}[\psi_B(\mathbf{r})-\psi_A(\mathbf{r})] \quad (5)$$

and maximization with respect to the effective pressure

$$\psi_+(\mathbf{r})=\tfrac{1}{2}[\psi_B(\mathbf{r})+\psi_A(\mathbf{r})]. \quad (6)$$

The SCFT equations defining the saddle point fields read[37,38]

$$\frac{\delta\mathcal{F}}{\delta\psi_+}=\varphi_A(\mathbf{r})+\varphi_B(\mathbf{r})-1=0,\quad \frac{\delta\mathcal{F}}{\delta\psi_-}=2f_A-1 + \frac{2}{\chi\mathcal{N}}\psi_-(\mathbf{r})+\varphi_B(\mathbf{r})-\varphi_A(\mathbf{r})=0, \quad (7)$$

where the local volume fractions $\varphi_A(\mathbf{r})$ and $\varphi_B(\mathbf{r})$ are given by the integrals

$$\varphi_i(\mathbf{r})=Q^{-1}(\{\psi_A,\psi_B\})\int_0^1 ds\sigma_i(s)q(\mathbf{r},s)\tilde{q}(\mathbf{r},1-s). \quad (8)$$

These equations identify $\varphi_A(\mathbf{r})$ and $\varphi_B(\mathbf{r})$ as the average densities of A and B chain segments at point $\mathbf{r}$ as calculated in an ensemble of noninteracting macromolecules subject to the fields $\psi_A(\mathbf{r})$ and $\psi_B(\mathbf{r})$ acting on A and B segments, respectively. The order parameter of the system is related to the difference between the densities of the two kinds of monomers. The end-segment distribution function $\tilde{q}(\mathbf{r},s)$, which appears in Eq. (8) and describes the opposite end of a chain

(from one to zero), is defined similar to Eq. (3),

$$\frac{\partial}{\partial s}\tilde{q}(\mathbf{r},s) = R_G^2\nabla^2\tilde{q}(\mathbf{r},s) - \psi(\mathbf{r},1-s)\tilde{q}(\mathbf{r},s), \tag{9}$$

with $\tilde{q}(\mathbf{r},0)=1$.

To solve Eqs. (1)–(9) for the two-length-scale multiblock copolymers under consideration, we suggested[36] to use the Ng iterative procedure.[39] (A somewhat abridged version of this procedure called Anderson mixing was used before to solve Eqs. (1)–(9) for diblock copolymer melts.[40])

In Ref. 36 this procedure was applied to 1D, 2D, and 3D morphologies in the region of not too high values of χ, where segregation inside the middle multiblock $(B_{N/2}A_{N/2})_n$ does not occur yet. In the present paper we apply this procedure to the lamellar 1D morphology only, which enables us to evaluate accurately 64 harmonics within a broader range of χ-values and, thus, to study the LL morphology formation.

To implement the Ng iteration scheme and find the (meta)stable periodic morphologies in this case, the following steps are to be done: (i) starting with some trial 1D periodic functions $\psi_\alpha(r)$ and initial conditions $q_\alpha(\mathbf{r},0)$ and $\tilde{q}_\alpha(\mathbf{r},0)$ to solve the diffusion Eqs. (3) and (9) with the corresponding periodic boundary conditions; (ii) with the solutions from step (i), to generate the single-chain partition function Q via Eq. (2); (iii) with the results of these two steps, to calculate the volume fractions $\varphi_\alpha(r)$'s via Eq. (8) and new self-consistent potentials $\psi_\alpha(r)$ via Eqs. (5)–(7) to be used for the next iteration; and (iv) to minimize the free energy functional Eq. (1) with respect to the imposed period D. Therewith, to solve the diffusion equations, which is the most expensive step in the calculation, the pseudospectral algorithm[38,41,42] is used as described in detail in Ref. 36. An important feature of our calculations, which improves considerably the convergence, is that we start in a vicinity of the critical point found precisely within the WST (Refs. 23–25) and use the WST data for the order parameter (composition) profile as an initial guess for the SCFT calculations (for more detail see Ref. 36). Then, increasing the χ-parameter we use the preceding solution as the next initial guess. This strategy results, as a rule, in converging to the global free energy minimum.

Of course, the iterative procedure could converge also to some other local free energy minima if we start from some special initial trial functions, which may be classified, e.g., by the number of local extrema of the order parameter profile per period. We believe, however, that if these minima differ from that obtained via the described procedure, they are only metastable. To check this hypothesis we applied the described iterative SCFT procedure for the multiblock $A_{20}(BA)_{10}$ copolymer melt considered in Ref. 26 using the following initial guess:

$$\psi_-^{(0)}(x) = C\left(w\left(\frac{x}{D}-\frac{1}{2},\eta,n\right)-w_0\right), \quad \psi_+^{(0)}(\mathbf{r})=0, \tag{10}$$

where C is a positive constant, D is the period, $1-\eta(0<\eta<1)$ is the volume fraction of the lamellar layers occupied by the A tails, the integer n is the number of local maxima within the period D, and w_0 is the average value of the function

$$w(t,\eta,n) = \begin{cases} [1-(-1)^n\cos(2\pi nt/\eta)]/2, & |t|<\eta/2, \\ 0, & \eta/2\le|t|\le 1/2, \end{cases} \tag{11}$$

within the interval of $-0.5\le t\le 0.5$. A typical trial function $\psi_-^{(0)}(x)$ is plotted in Fig. 4.

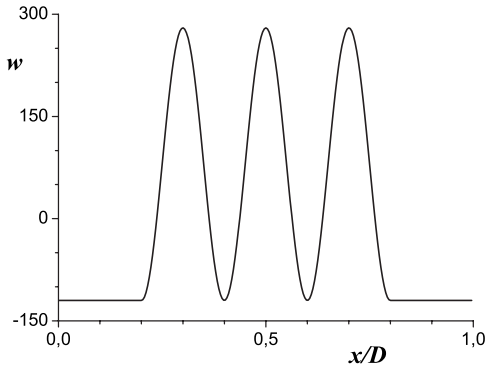

FIG. 4. A typical initial trial function [see Eq. (10)] specifying the profile topology for $n=3$ and $\eta=0.6$.

Given the topology of the solution specified by the value of n, the iterative procedure converges to some fixed point values $\eta=\eta^*$ and $D=D^*$, which provide the free energy minimum irrespective of the initial values $\eta=\eta_0$ and $D=D_0$ we start with. Comparing the thus calculated free energies for different n, we find that the solution providing the global free energy minimum is precisely the one found via the SCFT iterative procedure based on the WST initial guess and followed by using the preceding solution as the next initial guess.

III. RESULTS AND DISCUSSION

Thus, we applied the SCFT technique to study the LL formation in symmetric multiblock copolymers $A_{mN/2}(B_{N/2}A_{N/2})_nB_{mN/2}$ for $n=6$ and $m=0$, 1, 2, 3, 4, 5, 6, 7 and 8, which give a representative sample both in the LAM-S and LAM-L regions (see Fig. 3). Our main result presented in Fig. 5 is the dependence of the periods $D(n,m,\chi)$ measured in units of $R_G^{\mathrm{di}}=a\sqrt{N/6}$ on the reduced χ-parameter $\tilde{\chi}=\chi N$. The general trend of this dependence is rather nontrivial.

First of all, we clearly see two families of the $D(\chi)$ dependences: (i) the small-scale $(m=0,1,2)$ and large-scale $(m=3-8)$ ones, which agree well with the WST results discussed above. For the small-scale family D is close to unity. Therewith, the plots $D(\chi)$ for $m=0$ and 1 reveal a conventional[43] monotonic increase in D with increase in χ that corresponds to stretching of the blocks.[44–46] The values of $D(6,0,\chi)$ are somewhat higher than those of $D(6,1,\chi)\equiv D(7,0,\chi)$, where the latter identity follows from the fact that the structure with $n=6$ and $m=1$ is identical to that with $n=7$ and $m=0$ due to the very definition of the structural parameters n and m. Thus, the lamellar period for the tailless periodic multiblock copolymer melts $(A_{N/2}B_{N/2})_n$ decreases with increase in the number of diblocks n as shown

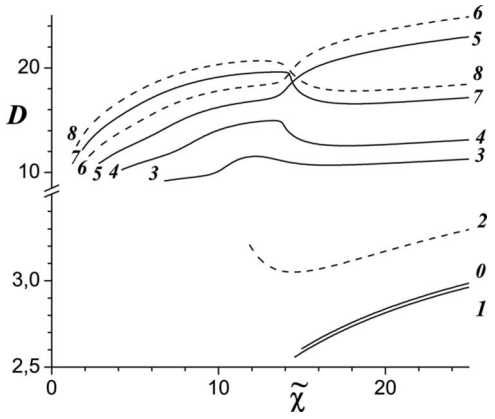

FIG. 5. The χ-dependence of the dimensionless lamellar morphology period D for various integer values of the relative tail length m at $n=6$ ($\tilde{\chi}=\chi N$). The solid curves zero and one correspond to the periods of the simple multiblock structures with $m=0$ and $m=1$ (or $n=7$ and $m=0$); the dashed line two corresponds to $m=2$. For the large-scale curves the lines are also labeled by the corresponding values of m. The curves six and eight are dashed to distinguish them from the close solid curves five and seven. The morphologies corresponding to $m=5$ and $m=6$ have two extra bilayers per period as compared to $m=3$, 4, 7, and 8.

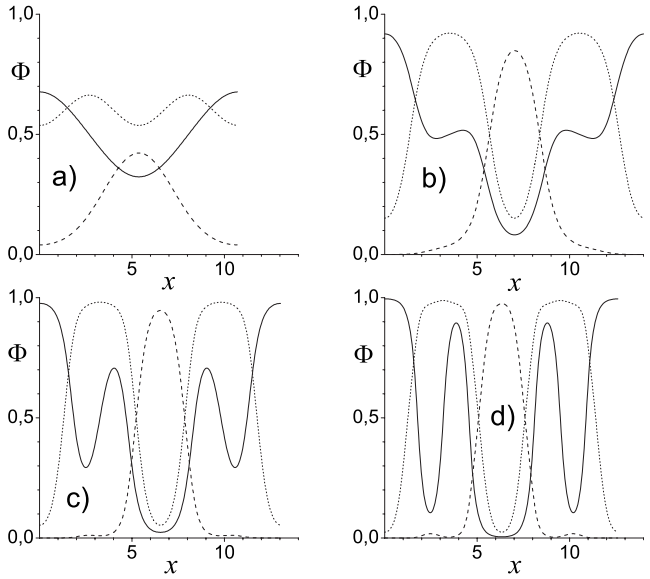

FIG. 6. The profiles of the total volume fraction of A monomers $\varphi_A(x)$ (solid) as well as the volume fractions $\tilde{\phi}_B(x)$ of the tails B (dotted) and $\phi_C(x)$ of the middle-block monomers (dashed) defined by Eqs. (12) and (13), respectively, for the case $n=6$ and $m=4$ at various degrees of segregation. (a) $\tilde{\chi}=\chi N=5$; (b) $\tilde{\chi}=10$; (c) $\tilde{\chi}=15$; and (d) $\tilde{\chi}=20$.

first via the random phase approximation.[47,48] For the first nontrivial tails ($m=2$), the starting period is somewhat larger than that for the multiblock copolymer $(A_{N/2}B_{N/2})_6$, therewith ordering starts for lower values of χ. Remarkably, in this case the initial evolution of the period with χ corresponds to a weak shrinking of the blocks rather than their stretching, the tendency being changed to normal stretching only from a finite level of segregation. Summarizing, our SCFT calculations do agree with the WST results (see Fig. 3), according to which these block copolymers belong to the LAM-S region.

For all other structures with $m \geq 3$ the plots $D(\chi)$ begin for considerably lower values of $\tilde{\chi}$ (there is no ordering yet for even lower values of $\tilde{\chi}$), the values of D being much bigger than unity, which is also consistent with the WST prediction of their large-length-scale (LAM-L) behavior. A new unexpected result we obtain within the SCFT is that the function $D(\chi)$ reveals a thresholdlike change in behavior, the threshold value being close to that of the ODT in the copolymer melt of the type $(B_{N/2}A_{N/2})_n$ (i.e., the multiblock middle part only). Remarkably, at the threshold both drastic increase and decrease in D are observed depending on the degree of polymerization of the long end blocks given by m: $D(\chi)$ drops for $m=3$, 4, 7, and 8 (an example of such a behavior has been already described by Nap *et al.*[26]) and jumps up for $m=5$ and 6.

To understand this unusual behavior it is worthy to remember that the system of interest is similar to the triblock ACB with the middle part $(B_{N/2}A_{N/2})_n$ playing the role of the middle nonselective block C. Close to the ODT, large-scale segregation between the long tails $A_{mN/2}$ and $B_{mN/2}$ occurs, the middle block being still disordered. No segregation occurs yet between the short A and B blocks that belong to the middle part $(B_{N/2}A_{N/2})_n$. However, such a segregation starts upon lowering the temperature at $\tilde{\chi}=\chi N \approx \tilde{\chi}_\infty^{\mathrm{ODT}}$ [here $\tilde{\chi}_\infty^{\mathrm{ODT}}$ is the reduced χ-parameter value[47] at the ODT for the multiblock copolymer melts $(B_{N/2}A_{N/2})_n$ in the limit $n \to \infty$]. It is this segregation that generates a LL structure as well as some striking conformational changes in the whole chain.

Indeed, the correlation between the changes in the period and overall appearance of the lamellar morphology is clearly seen in Fig. 6 where a typical evolution of the lamellar morphology for $m=4$ is presented. Here the total volume fraction $\varphi_A(x)$ of the monomers A, the volume fraction $\tilde{\phi}_B(x)$ of those monomers B that belong to the tails only, and the volume fraction $\phi_C(x)$ of both A and B monomers belonging to the middle multiblock part are plotted within one period, x being the coordinate along the axis normal to the layer plane measured in units R_G^{di}. $\varphi_A(x)$ is defined by Eq. (8) and similar equations hold for $\tilde{\phi}_B(x)$ and $\phi_C(x)$,

$$\tilde{\phi}_B(\mathbf{r}) = \frac{1}{Q[\psi_A,\psi_B]} \int_{1-\lambda}^{1} ds q(\mathbf{r},s)\tilde{q}(\mathbf{r},1-s), \tag{12}$$

$$\phi_C(\mathbf{r}) = \frac{1}{Q[\psi_A,\psi_B]} \int_{\lambda}^{1-\lambda} ds q(\mathbf{r},s)\tilde{q}(\mathbf{r},1-s), \tag{13}$$

where $\lambda = m/(2m+2n)$.

As is seen from Fig. 6, the fast drop in curve 4 in Fig. 5 is related to segregation within the multiblock middle part, which occurs upon lowering the temperature at $\tilde{\chi} \approx \tilde{\chi}_\infty^{\mathrm{ODT}}$. An even more impressive view on the distinction between the small- and large-scale behaviors as well as the difference between the two types of the large-scale plots in Fig. 5 provides the profiles of the total volume fraction $\varphi_A(x)$ of A monomers at $\tilde{\chi}=17$ (i.e., for a segregation higher than the threshold one) for various m shown in Fig. 7. We see that the block copolymers with $m \leq 2$, which reveal the small-scale behavior in Fig. 5, are characterized by comparatively simple profiles $\varphi_A(x)$ [see Figs. 7(a)–7(c)]. On the contrary, the block copolymers with $m \geq 3$ revealing the large-scale behavior in Fig. 5 are characterized by much more complex

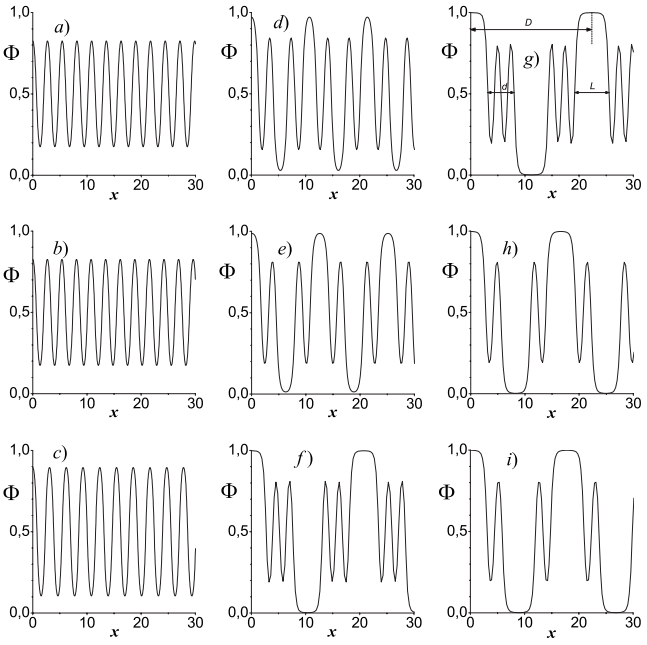

FIG. 7. The profiles of the total volume fraction of A monomers $\varphi_A(x)$, where the coordinate x along the axis normal to the layer plane is measured in units R_G^{di} for $n=6$ at $\tilde{\chi}=17$ and (a) $m=0$, (b) $m=1$, (c) $m=2$, (d) $m=3$, (e) $m=4$, (f) $m=5$, (g) $m=6$, (h) $m=7$, and (i) $m=8$. In (g) the definitions of the quantities D, L, and d introduced in Table I are visualized.

(LL) morphologies due to necessity to alternate the thick tail A and B layers and thin internal AB bilayers generated by segregation within the multiblock parts $(B_{N/2}A_{N/2})_n$.

It is also seen from Fig. 7 that the difference between the situations with a sharp swelling ($m=5$ and 6) and "shrinking" ($m=3$, 4, 7, and 8) of the LL morphologies is due to the fact that some extra AB bilayers are formed in the "swollen" morphologies (i.e., those having a comparatively bigger period D) by the middle multiblock parts (see also Fig. 8).

Additional information enabling comparison of the simple lamellar and LL morphologies is given in Table I. Here, as shown in Fig. 7, d and L are the widths of the layers[49] occupied basically by the middle part and the long tails, respectively, $d_0=2d/k$ is the (average) period of one small-length-scale AB bilayers, D is the period of the whole morphology, $h=L/m$ is a measure of the tail stretching, and $L/(L+d)$ is the spatial (length) fraction of the tail domains. Obviously, the quantities d, L, and h are defined for the LL morphologies only. Accordingly, the equalities $D=d_0$ and $D=2(L+d)$ hold (up to a round-off error) for the simple lamella and LL morphologies, respectively.

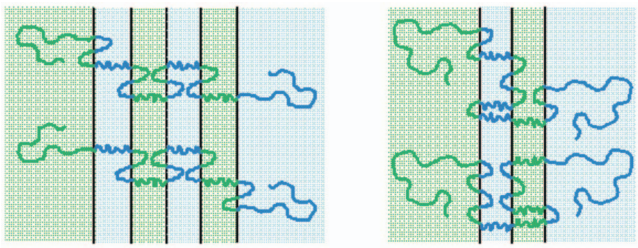

FIG. 8. (Color) Cartoons of the LL self-assembled state of $A_{mN/2}(B_{N/2}A_{N/2})_6B_{mN/2}$. Left: this situation corresponds to the case where the end blocks A and B are together five times ($m=5$) larger than the A and B blocks of the symmetric B-b-A blocks that form the middle multiblock. Right: here end blocks are eight times larger ($m=8$); however, the overall long period is smaller due to the formation of two rather than four internal layers.

The most transparent indicator, which distinguishes between the simple lamellar ($m=0$, 1, and 2) and both swollen ($m=5$ and 6) morphologies and shrunk ($m=3$, 4, 7, and 8) LL morphologies, is the number k of small-scale AB bilayers per morphology period: $k=1$, 2, and 4, respectively (accordingly, $d_0=d$ for all shrunk morphologies with $k=2$). One more useful indicator is the stretching h of the tails. Indeed, to form the swollen morphologies higher stretching is necessary as is clearly seen in Fig. 8, and for these morphologies the stretching of tails h is noticeably higher then for the shrunk ones. On the contrary, the widths d_0 of the thin bilayers within the LL morphologies somewhat decrease (see Table I) as compared to the trend revealed for the simple lamellas ($m=0-2$), which means that the internal blocks located in thin layers are somewhat compressed. Therewith, they are more compressed in swollen morphologies ($m=5$ and 6) than in the shrunk ones ($m=3$, 4, 7, and 8).

It is worthy to add the following observations. First, the fraction $L/(L+d)$ of the tail domains is higher than their mass ratio $m/(m+n)$, which witnesses that the short $A(B)$ blocks, which belong to the middle part and penetrate easily into the tail $A(B)$ domains (thus increasing their effective mass fraction), whereas the opposite does not hold. Second, the least stretching, which is observed for $m=7$, is correlated with a very good commensurability of the tail and multiblock domains. Finally, the period d_0 of the internal layers is oscillating with an increase in the tail length m, which resembles the oscillations of the period of the kinetically stable 1D spinodal decomposition patterns[50] and the lamellae in thin films[51] with change in the film width. Note that in our case the roles of the film width and the internal period belong to

TABLE I. The parameters of the lamellar-in-lamellar morphology ($n=6$, $\tilde{\chi}=17$).

m	$m/(m+n)$	k	d	d_0	L	h	D	$L/(L+d)$	D/d_0
0	0	1	⋯	2.714	⋯	⋯	2.714	⋯	1
1	1/7	1	⋯	2.691	⋯	⋯	2.691	⋯	1
2	1/4	1	⋯	3.089	⋯	⋯	3.089	⋯	1
3	1/3	2	2.748	2.748	2.604	0.868	10.701	0.487	3.896
4	2/5	2	2.735	2.735	3.551	0.888	12.570	0.565	4.596
5	5/11	4	4.915	2.457	5.449	1.090	20.736	0.526	8.435
6	1/2	4	4.840	2.420	6.336	1.056	22.353	0.567	9.235
7	7/13	2	2.772	2.772	5.542	0.791	16.625	0.667	5.999
8	4/7	2	2.761	2.761	6.163	0.770	17.851	0.691	6.462

the large period D of the overall lamellar structure and the width d_0 of one small-length-scale AB bilayer, respectively.

We believe these observations clearly witness the mutual self-adjusting between the WST large-scale period L_L and the small-scale period d_0 of the tailless multiblock copolymer $(A_{N/2}B_{N/2})_n$, which is to occur due to the fact that the overall profile $\varphi_A(x)$ is a periodic function.

IV. CONCLUSION

We have carried out the analysis of microphase separation in symmetric multiblock copolymer $A_{mN/2}(B_{N/2}A_{N/2})_nB_{mN/2}$ systems consisting of macromolecules with a specific architecture involving two different length scales. The pseudospectral algorithm we used[36] provides high precision to reveal both long and short scales of the separation. In the vicinity of the ODT weakly segregated lamellar phases are always observed. With an increase in the χ-parameter (and, thus, the domain segregation), two different types of the lamellar morphology could appear. For $m \leq 2$ the lamellar morphology formed is similar to that simple lamellar morphology, which occurs in linear multiblock copolymer melts $(A_{N/2}B_{N/2})_n$. For $m \geq 3$ the LL structures appear. The number of the internal layers k depends on the relative length m of the tails in a rather unusual nonmonotonic way, which is a consequence of the commensurability and self-adjusting effects between the small and large scales intrinsically present in the systems with two-length-scale architecture under consideration. We expect the commensurability effect described to be a rather general feature peculiar also for the 2D and 3D morphologies forming in copolymer melts with two-length-scale architecture.

ACKNOWLEDGMENTS

We thank for financial support the Dutch Organization for Scientific Research NWO (Grant No. 047.016.002) and Russian Federal Agency on Science and Innovations (Contract No. 02.513.11.3329). Y.A.K. and P.G.K. thank also the Russian Foundation for Basic Research (Grant No. 07-03-00385) and DFG (SFB 569). We thank an anonymous referee for making rather helpful comments.

[1] K. Binder, Adv. Polym. Sci. **138**, 1 (1999).
[2] M. J. Fasolka and A. M. Mayes, Annu. Rev. Mater. Res. **31**, 323 (2001).
[3] Q. Wang, in *Nanostructured Soft Matter*, edited by A. V. Zvelindovsky (Springer, Netherlands, 2007), pp. 495–527.
[4] H. J. Angerman, A. Johner, and A. N. Semenov, Macromolecules **39**, 6210 (2006).
[5] B. Miao, D. Yan, C. C. Han, and A.-C. Shi, J. Chem. Phys. **124**, 144902 (2006).
[6] I. Erukhimovich and A. Johner, Europhys. Lett. **79**, 56004 (2007).
[7] J. Ruokolainen, R. Mäkinen, M. Torkkeli, T. Mäkelä, R. Serimaa, G. ten Brinke, and O. Ikkala, Science **280**, 557 (1998).
[8] J. Ruokolainen, M. Saariaho, O. Ikkala, G. ten Brinke, E. L. Thomas, M. Torkkeli, and R. Serimaa, Macromolecules **32**, 1152 (1999).
[9] J. Ruokolainen, G. ten Brinke, and O. Ikkala, Adv. Mater. (Weinheim, Ger.) **11**, 777 (1999).
[10] O. Ikkala and G. ten Brinke, Science **295**, 2407 (2002).
[11] O. Ikkala and G. ten Brinke, Chem. Commun. (Cambridge) **2004**, 2131.
[12] G. ten Brinke, J. Ruokolainen, and O. Ikkala, Adv. Polym. Sci. **207**, 113 (2007).
[13] Y. Nagata, J. Masuda, A. Noro, D. Cho, A. Takano, and Y. Matsushita, Macromolecules **38**, 10220 (2005).
[14] J. Masuda, A. Takano, Y. Nagata, A. Noro, and Y. Matsushita, Phys. Rev. Lett. **97**, 098301 (2006).
[15] Y. Matsushita, Macromolecules **40**, 771 (2007).
[16] Y. Matsushita, Polym. J. (Tokyo, Jpn.) **40**, 177 (2008).
[17] A. F. Thünemann and S. General, Macromolecules **34**, 6978 (2001).
[18] I. W. Hamley, V. Casteletto, P. Parras, Z. B. Lu, C. T. Imrie, and T. Itoh, Soft Matter **1**, 353 (2005).
[19] S. Hanski, N. Houbenov, J. Ruokolainen, D. Chondronicola, H. Iatrou, N. Hadjichristidis, and O. Ikkala, Biomacromolecules **7**, 3379 (2006).
[20] M. J. Birnkrant, C. Y. Li, L. V. Natarajan, V. P. Tondiglia, R. L. Sutherland, P. F. Lloyd, and T. J. Bunning, Nano Lett. **7**, 3128 (2007).
[21] R. Nap, C. Kok, G. ten Brinke, and S. Kuchanov, Eur. Phys. J. E **4**, 515 (2001).
[22] R. Nap and G. ten Brinke, Macromolecules **35**, 952 (2002).
[23] Yu. G. Smirnova, G. ten Brinke, and I. Ya. Erukhimovich, Polym. Sci., A Ser. A Ser. B **47**, 740 (2005).
[24] Yu. G. Smirnova, G. ten Brinke, and I. Ya. Erukhimovich, J. Chem. Phys. **124**, 054907 (2006).
[25] Yu. G. Smirnova, "Microphase separation in two-length-scale multiblock copolymer melts," Ph.D. thesis, Rijksuniversiteit Groningen, 2006.
[26] R. Nap, N. Sushko, I. Erukhimovich, and G. ten Brinke, Macromolecules **39**, 6765 (2006).
[27] A. Subbotin, T. Klymko, and G. ten Brinke, Macromolecules **40**, 2915 (2007).
[28] T. Klymko, A. Subbotin, and G. ten Brinke, J. Chem. Phys. **129**, 114902 (2008).
[29] T. Klymko, T. V. Markov, A. Subbotin, and G. ten Brinke, Soft Matter **5**, 98 (2009).
[30] M. W. Matsen and M. Schick, Phys. Rev. Lett. **72**, 2660 (1994).
[31] M. W. Matsen and F. S. Bates, Macromolecules **29**, 1091 (1996).
[32] L. Leibler, Macromolecules **13**, 1602 (1980).
[33] S. Kuchanov, V. Pichugin, and G. ten Brinke, Europhys. Lett. **76**, 959 (2006).
[34] I. Y. Erukhimovich, Eur. Phys. J. E **18**, 383 (2005).
[35] C. A. Tyler, J. Qin, F. S. Bates, and D. C. Morse, Macromolecules **40**, 4654 (2007).
[36] Yu. A. Kriksin, I. Ya. Erukhimovich, P. G. Khalatur, Yu. G. Smirnova, and G. ten Brinke, J. Chem. Phys. **128**, 244903 (2008).
[37] G. H. Fredrickson, *The Equilibrium Theory of Inhomogeneous Polymers* (Oxford University Press, Oxford, 2006).
[38] H. D. Ceniceros and G. H. Fredrickson, Multiscale Model. Simul. **2**, 452 (2004).
[39] K.-C. Ng, J. Chem. Phys. **61**, 2680 (1974).
[40] R. B. Thompson, K. Ø. Rasmussen, and T. Lookman, J. Chem. Phys. **120**, 31 (2004).
[41] M. D. Feit, J. A. Fleck, and A. Steiger, J. Comput. Phys. **47**, 412 (1982).
[42] K. O. Rasmussen and G. Kalosakas, J. Polym. Sci., Part B: Polym. Phys. **40**, 1777 (2002).
[43] K. Almdal, J. H. Rosedale, F. S. Bates, G. D. Wignall, and G. H. Fredrickson, Phys. Rev. Lett. **92**, 6255 (1990).
[44] H. Fried and K. Binder, Europhys. Lett. **16**, 237 (1991).
[45] J. L. Barrat and G. H. Fredrickson, J. Chem. Phys. **95**, 1281 (1991).
[46] I. Ya. Erukhimovich and A. V. Dobrynin, Macromolecules **25**, 4411 (1992).
[47] I. Ya. Yerukhimovich, Polym. Sci. U.S.S.R. **24**, 2232 (1982).
[48] H. Benoit and G. Hadziioannou, Macromolecules **21**, 1449 (1988).
[49] The widths of the layers are calculated as the distances along the normal to the lamellar layers between the intermaterial dividing surfaces (the lamellar cross-sections with the values of $\varphi_A(x)$ equal to 0.5).
[50] V. S. Mitlin, L. I. Manevich, and I. Ya. Erukhimovich, Sov. Phys. JETP **61**, 290 (1985).
[51] P. Lambooy, T. P. Russell, G. J. Kellogg, A. M. Mayes, P. D. Gallagher, and S. K. Satija, Phys. Rev. Lett. **72**, 2899 (1994).